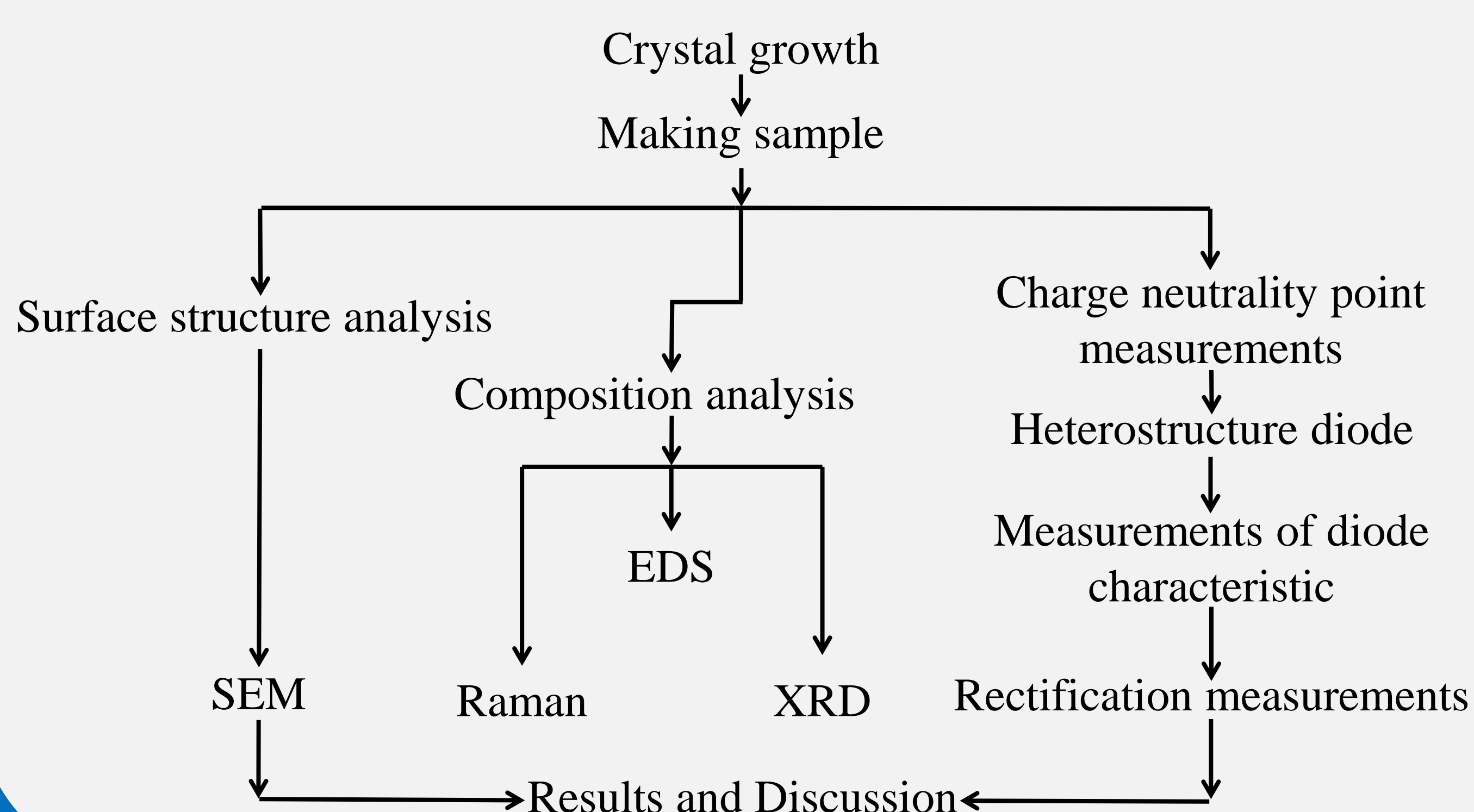


Growth and Electrical Characteristics of $\text{Mo}_{1-x}\text{W}_x\text{S}_2$ ($0 \leq x \leq 1$) Crystals

Abstract

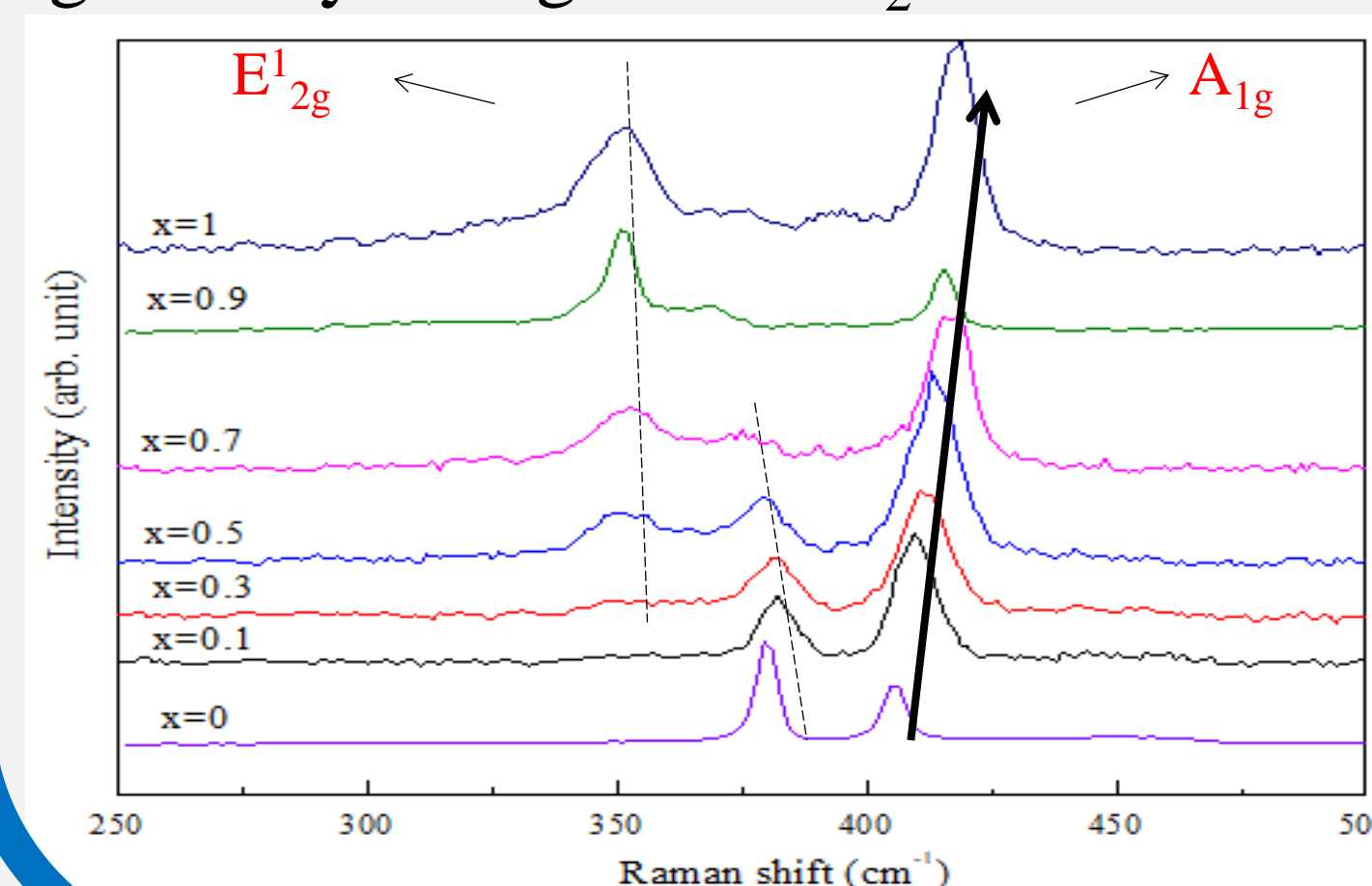
We used chemical vapor transport (CVT) to prepare $\text{Mo}_{1-x}\text{W}_x\text{S}_2$ with different crystal contents, and obtained 3 to 5 μm thick materials from the crystal by mechanical exfoliation. By scanning electron microscopy (SEM), energy dispersive X-ray spectroscopy (EDX), Raman spectroscopy, X-ray diffraction (XRD) and field effect transistor (FET) detection, we found that different X concentrations of $\text{Mo}_{1-x}\text{W}_x\text{S}_2$ materials have different values. In the study, MoS_2 was vertically stacked with different X concentrations of $\text{Mo}_{1-x}\text{W}_x\text{S}_2$ material to form a diode, and a series of electrical measurements were performed. We observed different pn or nn features. The diode measurements and the rectification characteristics work successfully at different frequencies.

Experiment Process



Raman

Fig. 3 shows the $\text{Mo}_{1-x}\text{W}_x\text{S}_2$ Raman plots for different X concentrations. The E_{2g}^1 of MoS_2 gradually disappeared. The E_{2g}^1 of WS_2 gradually increased, indicating that with the increase of X content, MoS_2 gradually changed to WS_2 .



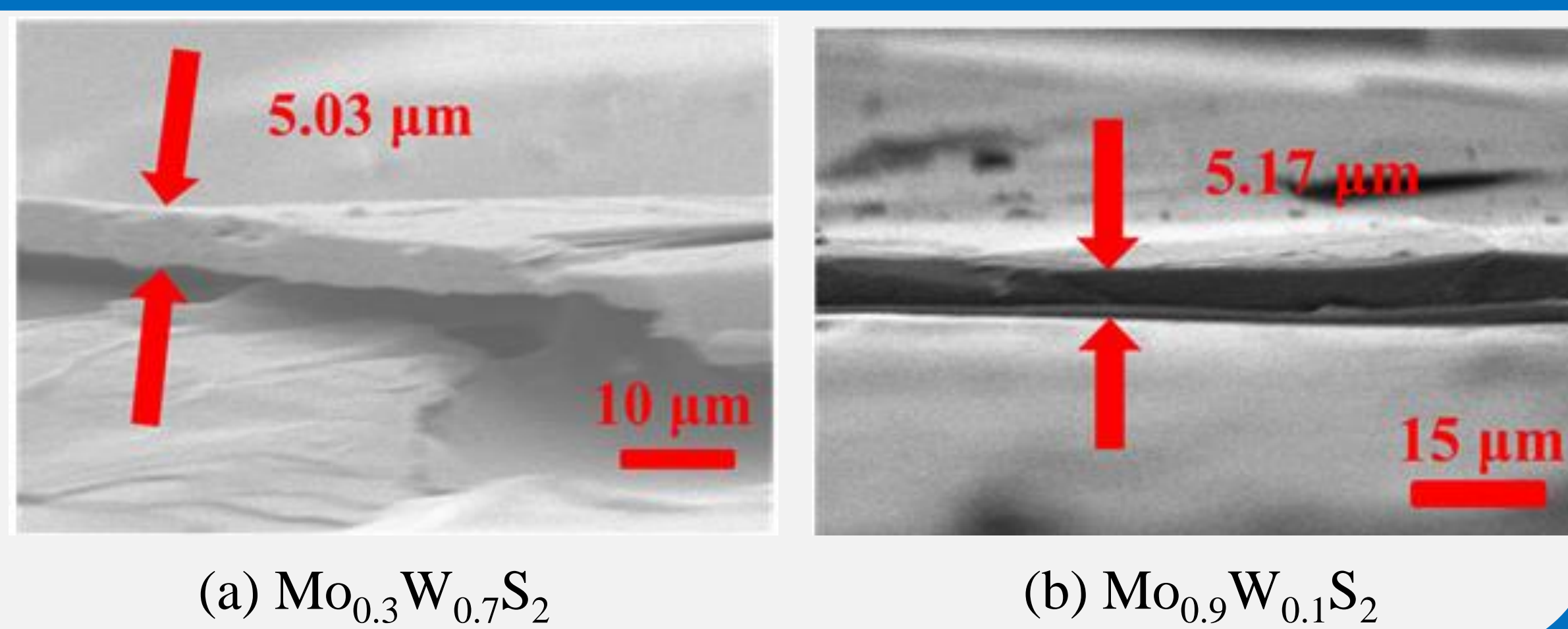
EDX

Table 1 is a ratio of $\text{Mo}_{1-x}\text{W}_x\text{S}_2$ elements measured by EDX, and it was found that the $\text{Mo}_{1-x}\text{W}_x\text{S}_2$ series single crystals were successfully mixed into MoS_2 at different ratios.

Sample	Mo(%)	W(%)	S(%)
MoS_2	33.44	0.00	66.56
$\text{Mo}_{0.9}\text{W}_{0.1}\text{S}_2$	29.26	6.54	64.20
$\text{Mo}_{0.7}\text{W}_{0.3}\text{S}_2$	24.28	11.20	64.52
$\text{Mo}_{0.5}\text{W}_{0.5}\text{S}_2$	23.44	17.21	59.35
$\text{Mo}_{0.3}\text{W}_{0.7}\text{S}_2$	13.73	23.70	62.57
$\text{Mo}_{0.1}\text{W}_{0.9}\text{S}_2$	5.02	29.62	65.36
WS_2	0.00	33.52	66.48

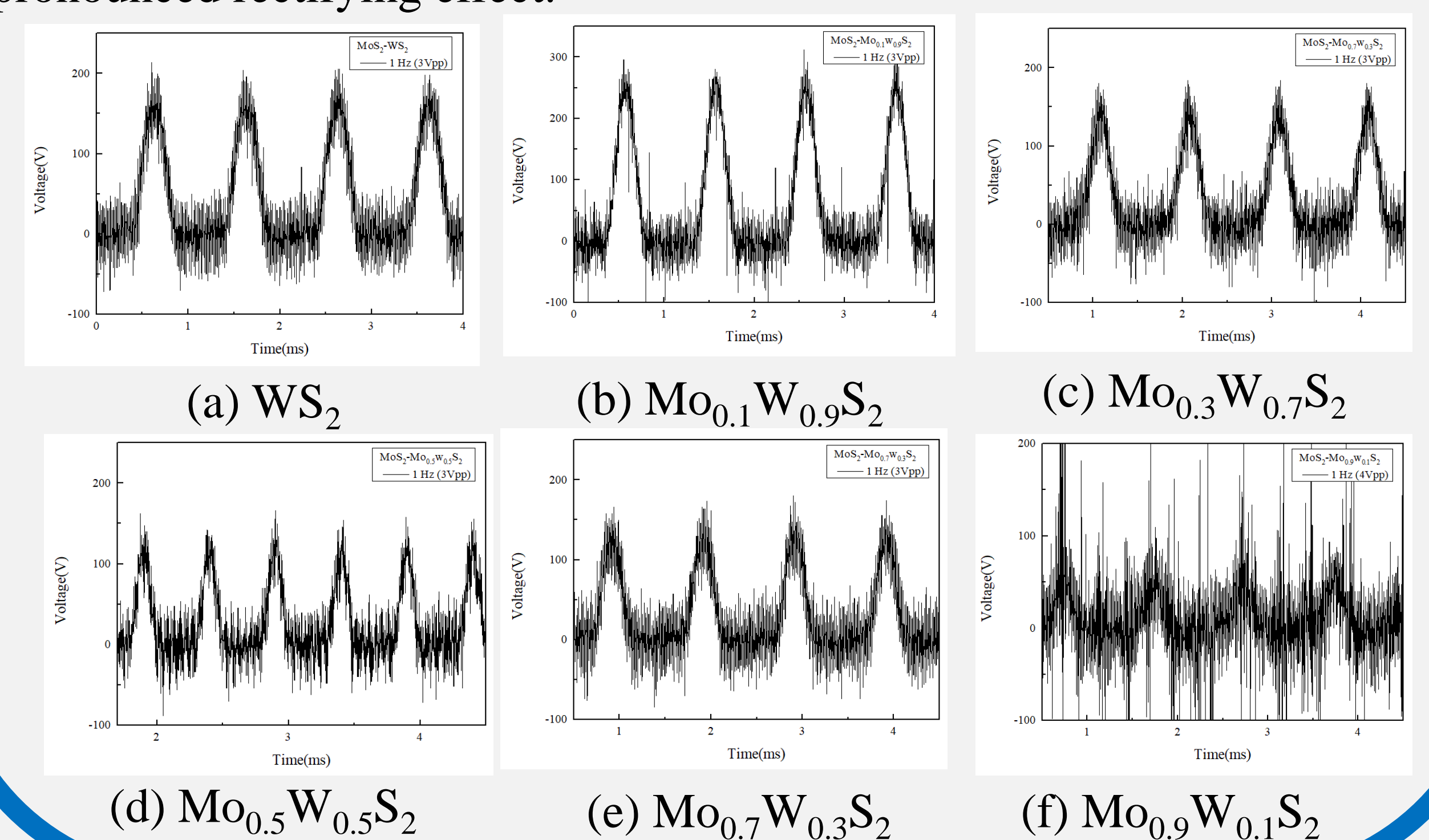
SEM

Fig. 1 shows the thickness of the $\text{Mo}_{1-x}\text{W}_x\text{S}_2$ sample as measured by SEM, eliminating the effect of thickness on the experiment.



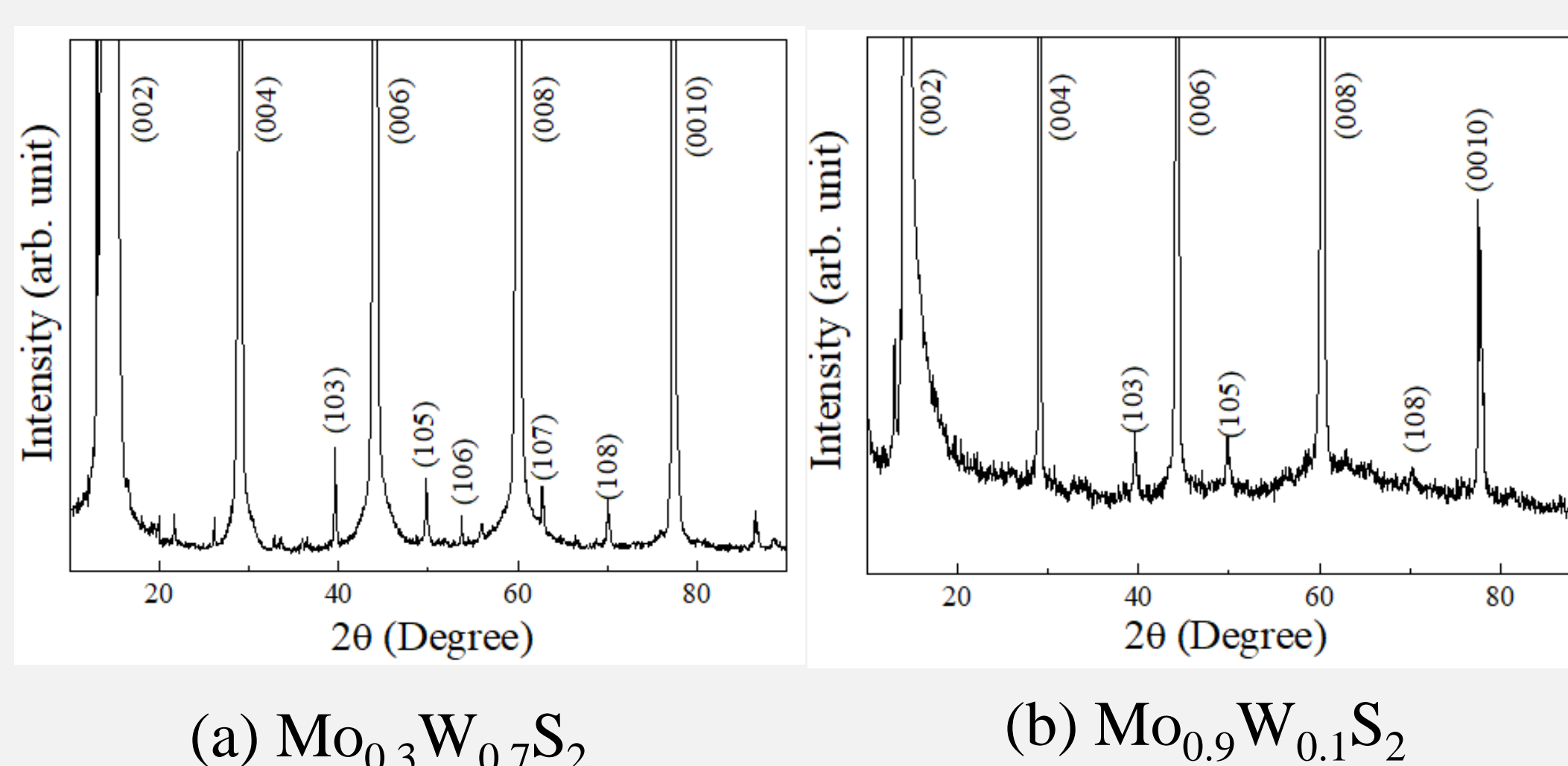
Rectification

Fig. 5 shows the rectification mode of $\text{MoS}_2\text{-Mo}_{1-x}\text{W}_x\text{S}_2$ (3 Vpp-1 Hz). We found that the $\text{Mo}_{1-x}\text{W}_x\text{S}_2$ and MoS_2 produced by CVT, the fabricated pn and nn diodes can be rectified in a low frequency environment, and the lower the X concentration, the more complete the rectification effect and can be maintained in a relatively high frequency environment. When the X concentration is higher, a larger voltage is required to have a more pronounced rectifying effect.



XRD

Fig. 2 shows the $\text{Mo}_{1-x}\text{W}_x\text{S}_2$ X-ray diffraction pattern. The measured Miller index is consistent with the JCPDS database. Since the WS_2 peaks (106) and (107) are larger than MoS_2 , it can be seen from the results that the $\text{Mo}_{0.3}\text{W}_{0.7}\text{S}_2$ (106) and (107) peaks cannot be seen in $\text{Mo}_{0.9}\text{W}_{0.1}\text{S}_2$.



Conclusions

Through various measurements, we successfully produced $\text{Mo}_{1-x}\text{W}_x\text{S}_2$ with high quality and layered structure, and measured the characteristics of pn and nn diodes by vertical stacking. All measurement results are consistent with the literature, and by observing the rectification pattern, we understand both the p-type or n-type $\text{Mo}_{1-x}\text{W}_x\text{S}_2$ diodes have a rectifying effect after being stacked with MoS_2 . And the lower the X concentration, the $\text{Mo}_{1-x}\text{W}_x\text{S}_2$ can be rectified in a relatively high frequency environment. The larger the difference in pn polarity, the better the rectification effect.

I-V curve

Fig. 4 shows that the I-V curve results of the overlap of $\text{Mo}_{0.3}\text{W}_{0.7}\text{S}_2$ and $\text{Mo}_{0.9}\text{W}_{0.1}\text{S}_2$ with MoS_2 are consistent with the literature.

